


# Rapid decline in MyHC I( $\beta$ ) mRNA expression in rat soleus during hindlimb unloading is associated with AMPK dephosphorylation

Natalia A. Vilchinskaya<sup>1</sup>, Ekaterina P. Mochalova<sup>1</sup>, Tatiana L. Nemirovskaya<sup>1,2</sup>, Timur M. Mirzoev<sup>1</sup> , Olga V. Turtikova<sup>1</sup> and Boris S. Shenkman<sup>1</sup>

<sup>1</sup>Myology Laboratory, Institute of Biomedical Problems RAS, Moscow, Russia

<sup>2</sup>Faculty of Basic Medicine, Lomonosov Moscow State University, Moscow, Russia

Edited by: Scott Powers and Karyn Hamilton

## Key points

- Inactivation of a skeletal muscle results in slow to fast myosin heavy chain (MyHC) shift.
- AMP-activated protein kinase (AMPK) can be implicated in the regulation of genes encoding the slow MyHC isoform.
- Here we report that AMPK dephosphorylation after 24 h of mechanical unloading can contribute to histone deacetylase (HDAC) nuclear translocation; activation of AMPK prevents HDAC4 nuclear accumulation after 24 h of unloading and AMPK dephosphorylation inhibits slow MyHC expression following 24 h of unloading.
- Our data indicate that AMPK dephosphorylation during the first 24 h of mechanical unloading has a significant impact on the expression of MyHC isoforms in rat soleus causing a decrease in MyHC I( $\beta$ ) pre-mRNA and mRNA expression as well as MyHC IIA mRNA expression.

**Abstract** One of the key events that occurs during skeletal muscle inactivation is a change in myosin phenotype, i.e. increased expression of fast isoforms and decreased expression of the slow isoform of myosin heavy chain (MyHC). It is known that calcineurin/nuclear factor of activated T-cells and AMP-activated protein kinase (AMPK) can regulate the expression of genes encoding MyHC slow isoform. Earlier, we found a significant decrease in phosphorylated AMPK in rat soleus after 24 h of hindlimb unloading (HU). We hypothesized that a decrease in AMPK phosphorylation and subsequent histone deacetylase (HDAC) nuclear translocation can be one of the triggering events leading to a reduced expression of slow MyHC. To test this hypothesis, Wistar rats were treated with AMPK activator (AICAR) for 6 days before HU as well as during 24 h of HU. We discovered that AICAR treatment prevented a decrease in pre-mRNA and mRNA expression of MyHC I as well as MyHC IIA mRNA expression. Twenty-four hours of hindlimb suspension resulted in HDAC4 accumulation in the nuclei of rat soleus but AICAR pretreatment prevented this accumulation. The results of the study indicate that AMPK dephosphorylation after 24 h of HU had a significant impact on the MyHC I and MyHC IIA mRNA expression in rat soleus. AMPK dephosphorylation also contributed to HDAC4 translocation to the nuclei of soleus muscle fibres, suggesting an important role of HDAC4 as an epigenetic regulator in the process of myosin phenotype transformation.

(Resubmitted 28 August 2017; accepted after revision 29 September 2017; first published online 3 October 2017)

**Corresponding author** T. M. Mirzoev: Institute of Biomedical Problems RAS, Myology Laboratory, 123007, Khoroshevskoe shosse 76A, Moscow, Russian Federation. Email: tmirzoev@yandex.ru

## Introduction

One of the key events that occurs during skeletal muscle inactivation/unloading is a change in myosin phenotype, i.e. increased expression of fast isoforms and decreased expression of the slow isoform of myosin heavy chain (MyHC) (Pette & Staron, 2001). A significant decrease in MyHC I mRNA expression in rat soleus muscle has been observed as early as 1 day following hindlimb unloading (HU) (Giger *et al.* 2009). It is known that the calcineurin–nuclear factor of activated T-cells (NFAT) pathway as well as AMP-activated protein kinase (AMPK) can regulate the expression of the *Myh7* gene encoding slow-type MyHC (Liu *et al.* 2014). The downregulation of *Myh7* gene expression may be the consequence of calcineurin inhibition or increased NFATc1 phosphorylation and efflux from myonuclei associated with glycogen synthase kinase 3 $\beta$  (GSK3 $\beta$ ) inactivation/negative phosphorylation (Shen *et al.* 2007). However, the GSK3 $\beta$  phosphorylation level did not differ from the control level after 24 h of HU (Mirzoev *et al.* 2016). Calcineurin-2 (myozenin-1; a calcineurin inhibitor) mRNA expression remained unchanged after 24 h of HU (the authors' unpublished observation). Therefore, we do not believe that alteration of calcineurin/NFATc1 pathway can be involved in the MyHC I downregulation observed by Giger *et al.* (2009) after 24 h of HU. We suppose that the epigenetic effects of Class IIA histone deacetylase (HDAC) phosphorylation/dephosphorylation and cytoplasmic–nuclear traffic may be involved (Liu *et al.* 2005). HDAC4 and 5 may be the target of several protein kinases, including AMPK (Röckl *et al.* 2007). Until recently, the issue of AMPK phosphorylation in soleus muscle under conditions of mechanical unloading has been disputed. Indeed, Hilder *et al.* (2005) and Han *et al.* (2007) have reported opposite data on the level of AMPK phosphorylation in rat soleus after 14 days' HU. Egawa *et al.* (2015) did not find any changes in AMPK phosphorylation as well as in acetyl-CoA carboxylase (ACC) phosphorylation levels in murine soleus muscle after 10 days of hindlimb unloading. Recently, we have found a significant decrease in the content of phosphorylated AMPK in rat soleus after 24-h HU (Mirzoev *et al.* 2016). A similar decrease in AMPK phosphorylation was observed in human soleus muscle following a 3-day exposure to unloading via dry immersion (Vilchinskaya *et al.* 2015). However, we observed the return of AMPK phosphorylation levels to the control values after 7 days' unloading (Mirzoev *et al.* 2016). AMPK phosphorylation can be induced by calcium/calmodulin-dependent protein kinase kinase 2 and liver kinase B1, but most authors believe that AMPK activation is allosterically regulated by alterations in the ratio of dephosphorylated and phosphorylated high-energy phosphates (Mounier *et al.* 2015). We can assume that

the lack of contractile activity of the soleus muscle under support withdrawal (De-Doncker *et al.* 2005) causes a rapid accumulation of phosphorylated high-energy phosphates (ATP, ADP and creatine phosphate) and leads to a reduced AMPK activity. In a rat study, Putman *et al.* (2015) showed that changes in the ratio of intracellular high-energy phosphates can induce changes in the myosin phenotype of muscle fibres. Matoba and co-authors (1993) managed to prevent a reduction in the slow-type MyHC in skeletal muscle of unloaded rats by  $\beta$ -guanidinopropionic acid, which shifted the balance of adenine nucleotides towards their dephosphorylated forms (AMP and ADP). It has been shown that  $\beta$ -guanidinopropionic acid's effects are mediated by increased levels of AMPK phosphorylation (Zong *et al.* 2002). It is known that AMPK can phosphorylate HDAC4 and HDAC5, which, in turn, can facilitate the expression of slow-type MyHC and a number of genes controlling regulatory proteins of oxidative metabolism (Röckl *et al.* 2007; McGee & Hargreaves 2010). Indeed, it has been shown that HU induced an increase in histone H3 acetylation at the type IIb (fast) MyHC (Pandorf *et al.* 2009). Recently, Dupré-Aucouturier *et al.* (2015) have found that trichostatin A (HDAC inhibitor) treatment leads to a significant reduction in unloading-induced muscle atrophy preventing slow-to-fast fibre transformation. Therefore, a decrease in AMPK phosphorylation and subsequent HDAC translocation to the nuclei would be one of the triggering events leading to the reduced expression of slow-type MyHC. To test this hypothesis it is necessary to exclude any decrease in the content of phosphorylated AMPK within 24 h of HU. For this purpose, we used a specific AMPK stimulator, 5-aminoimidazole-4-carboxamide ribofuranoside (AICAR). The negative modulation of AMPK abundance during unloading (using of AMPK-negative mutants and knockouts) will not help to reveal the functional link between AMPK dephosphorylation and downstream signalling events at the early stage of unloading. The study aimed to analyse the functional changes of AMPK activities and their consequences, not the impact of AMPK abundance. Moreover, it cannot be excluded that in the AMPK-deficient animals a different MyHC-driving mechanism might be hyperactive. However, some authors reported that the introduction of AICAR to intact rats does not significantly increase AMPK phosphorylation in the soleus muscle (Zheng *et al.* 2001). Our aim was to prevent any reduction in AMPK activity during the first 24 h of HU. Therefore, we applied a pretreatment of animals with AICAR injections. If our hypothesis is correct, then pretreatment of rats with AICAR before and during 24-h HU would maintain the level of AMPK phosphorylation, prevent an increase in HDAC4 content in the nuclei as well as facilitate MyHC I( $\beta$ ) expression in rat soleus muscle.

The results of the present study have fully confirmed our hypothesis.

## Methods

### Ethical approval

All procedures with animals were approved by the Biomedicine Ethics Committee of the Institute of Biomedical Problems of the Russian Academy of Sciences/Physiology section of the Russian Bioethics Committee (protocol no. 414, 23.12.2015). All experiments were performed in strict accordance with the guidelines and recommendations described by Grundy (2015). All efforts were made to minimize the animals' pain and suffering. Animals were housed in a temperature-controlled room on a 12:12 h light–dark cycle with food pellets and water provided *ad libitum*. Thirty-two 3-month-old male Wistar rats ( $190 \pm 5$  g) were obtained from the certified Nursery for laboratory animals of the Institute of Bioorganic Chemistry of the Russian Academy of Sciences (Pushchino, Moscow region). Prior to all surgical procedures, the animals were anaesthetized with an intraperitoneal injection of tribromoethanol ( $240 \text{ mg kg}^{-1}$ ). The depth of anaesthesia was evaluated by testing the pedal withdrawal reflex (toe and foot pad pinch).

### Experimental design and AICAR treatment

Unloading of the hindlimbs was induced by using a standard rodent hindlimb suspension/unloading model (Morey-Holton & Globus, 2002), following the recommendations provided by the European Convention for the protection of Vertebrate Animals used for Experimental and Scientific purposes (Council of Europe number 123, Strasbourg, 1985). Briefly, a strip of adhesive tape was applied to the animal's tail, which was suspended by passing the tape through a swivel that was attached to a metal bar on the top of the cage. This allowed the forelimbs to have contact with the grid floor and allowed the animals to move around the cage for free access to food and water. The suspension height was adjusted to prevent the hindlimbs from touching any supporting surface while maintaining a suspension angle of approximately 30 deg. The animals were randomly assigned to the following groups ( $n = 8/\text{group}$ ): (1) cage control (C); (2) control + AICAR (CA); (3) 24-h hindlimb suspension (HS); (4) 24-h HS + AICAR (HSA). Animals from the CA and HSA groups were daily treated with AICAR (Toronto Research Chemicals, Canada) 6 days before HS and 1 day during 24-h HS. Intraperitoneal AICAR injections were given at a dose of  $400 \text{ mg kg}^{-1}$ . The rats from the C and HS groups were treated with an equivalent dose of saline. Under anaesthesia, soleus muscles from control and unloaded rats were surgically excised from both hindlimbs, blotted

on filter paper, trimmed of their tendons, frozen in liquid nitrogen, and stored at  $-80^\circ\text{C}$  until further analysis. After muscle excision, the rats were killed by a tribromoethanol overdose (i.p.) followed by cervical dislocation.

**Western blot analysis.** Cytoplasmic and nuclear protein fractions from skeletal muscle tissue were separated and isolated using an NE-PER Nuclear and Cytoplasmic Extraction kit (Thermo Fisher Scientific, Waltham, MA, USA) following the manufacturer's instructions. For SDS-PAGE,  $10 \mu\text{g}$  (for nuclear fraction) or  $20 \mu\text{g}$  (for cytoplasmic fraction) of protein was loaded and separated on a 10% polyacrylamide gel, followed by transfer to a  $0.45 \mu\text{m}$  nitrocellulose membrane (Bio-Rad Laboratories, Hercules, CA, USA) by electroblotting. Then, to verify equal loading of protein in all lanes, the nitrocellulose membrane was dyed by Ponceau S. The membranes were blocked for 1 h at room temperature with the blocking buffer (TBS-T: 4% non-fat milk powder; Tris-buffered saline, pH 7.4; and 0.1% Tween 20) and incubated overnight at  $4^\circ\text{C}$  with primary antibodies (diluted in TBS-T) against p-AMPK $\alpha$ 1/2 (Thr 172, 1:500; Santa Cruz Biotechnology, Dallas, TX, USA, no. 33524), p-AMPK $\alpha$ 1/2 (Ser 485/491, 1:500, Cell Signaling Technology, Danvers, MA, USA, no. 4185), t-AMPK (1:500, Cell Signaling Technology, no. 2532), p-ACC (Ser 79, 1:1000, Cell Signaling Technology, no. 3661), t-ACC (1:2000, Cell Signaling Technology, no. 3662), p-PKD (Ser 916, 1:500, Cell Signaling, no. 2051), HDAC4 (1:500, Cell Signaling, no. 2072), HDAC5 (1:5000, Abcam, Cambridge, MA, USA, ab1439), PGC-1 $\alpha$  (1:2000, Abcam, ab54481), lamin B1 (1:500, Abcam, ab16048) and glyceraldehyde-3-phosphate dehydrogenase (GAPDH, 1:10000; Applied Biological Materials Inc., Richmond, British Columbia, Canada, no. G041). Three 10-min washes with TBS-T were then performed. After that, the membranes were incubated for 1 h at room temperature with horseradish peroxidase-conjugated secondary antibodies to rabbit or mouse immunoglobulins (1:4000, Santa Cruz Biotechnology). The membranes were then washed again in TBS-T 3 times for 10 min and incubated in the Immuno-Star HRP Chemiluminescent system (Bio-Rad Laboratories). The protein bands were quantified using a C-DiGit Blot Scanner (LI-COR Biotechnology, Lincoln, NE, USA) and Image Studio C-DiGit software. The signal from the protein bands was normalized to total protein, GAPDH or lamin B.

**RT-PCR analysis.** Reverse transcription was performed by incubation of  $0.5 \mu\text{g}$  of RNA, random hexamers d(N)6, dNTPs, RNase inhibitor and Moloney Murine Leukemia Virus (M-MLV) (Sintol, Moscow, Russia) reverse transcriptase for 60 min at  $37^\circ\text{C}$ . Samples to be compared were run under similar conditions (template amounts, duration of PCR cycles). The annealing

**Table 1. Primers used for RT-PCR analysis**

| Gene description | Forward primer/reverse primer                                    | GenBank        |
|------------------|------------------------------------------------------------------|----------------|
| Cyclophilin A    | 5'-AGCACTGGGGAGAAAGGATT-3'<br>5'-AGCCACTCAGTCTTGGCAGT-3'         | NM_017101.1    |
| <i>Rpl19</i>     | 5'-GTACCCTTCTTCCCTATGC-3'<br>5'-CAATGCCAACTCTCGTCAACAG-3'        | NM_031103.1    |
| <i>Actb</i>      | 5'-TCATGAAGTGTGACGTTGACATCC-3'<br>5'-GTA AACGCAGCTCAGTAACAGTC-3' | NM_031144.3    |
| <i>Gapdh</i>     | 5'-ACGGCAAGTTCACGGCACAGTCAA-3'<br>5'-GCTTCCAGAGGGGCCATCCACA-3'   | NM_017008.4    |
| <i>Ppargc1a</i>  | 5'-CTGCCATTGTTAAGACCGAGAA-3'<br>5'-ACTGCGGTTGTGTATGGACTT-3'      | NM_031347.1    |
| <i>Myh7</i>      | 5'-ACAGAGGAAGACAGGAAGAACCTAC-3'<br>5'-GGGCTTACAGGCATCCTTAG-3'    | NM_017240.2    |
| <i>Myh2</i>      | 5'-TATCCTCAGGCTCAAGATTTG-3'<br>5'-TAAATAGAATCACATGGGGACA-3'      | NM_001135157.1 |
| <i>Myh4</i>      | 5'-CTGAGGAACAATCCAACGTC-3'<br>5'-TTGTGTGATTTCTTCTGCACCT-3'       | NM_019325.1    |
| <i>Myh1</i>      | 5'-CGCGAGGTTACACCAA-3'<br>5'-TCCCAAAGTGTAAAGTACAAAATGG-3'        | NM_001135158.1 |
| pre- <i>Myh7</i> | 5'-ACTTAGCAGGCAAATCTCAGTAGC-3'<br>5'-CTCGGTTATGTTTCTCATCCGAAT-3' | NM_017240.2    |

temperature was based on the PCR primers' optimal annealing temperature. PCR primers used for RNA analysis are shown in Table 1. The amplification was real time monitored using SYBR Green I dye and the iQ5 Multicolour Real-Time PCR Detection System (Bio-Rad Laboratories). To confirm the amplification specificity, the PCR products from each primer pair were subjected to a melting curve analysis and sequencing of the products was provided at least once. Relative quantification was performed based on the threshold cycle ( $C_T$  value) for each of the PCR samples (Livak & Schmittgen, 2001). RPL19,  $\beta$ -actin, cyclophilin A and GAPDH were tested and chosen for the normalization of all quantitative PCR analysis experiments in the current study.

**Statistical analysis.** All data are expressed as median and interquartile range (0.25–0.75). Statistical analysis was performed using the REST 2009 v.2.0.12 (Qiagen, Germany) and Origin Pro v.8.0 (OriginLab Corp., Northampton, MA, USA) programs. Since the data were not normally distributed, a nonparametric Kruskal–Wallis test was used, and *post hoc* analysis was performed using Dunn's multiple range test with  $P < 0.05$  designated as statistically significant.

## Results

In the intact animals pretreated with AICAR there was a tendency towards an increase in the content of phosphorylated AMPK (Thr 172) ( $P = 0.09$ ) vs. the C group (Fig. 1A). In the HS group there was a significant

decrease ( $P < 0.05$ ) in the content of phosphorylated AMPK (Thr 172) by 33% vs. the C group (Fig. 1A). In the HSA group we did not observe any significant difference in the level of AMPK phosphorylation (Thr 172) compared to the C group (Fig. 1A). The content of phosphorylated AMPK (Thr 172) was higher in the HSA group compared to the HS group (Fig. 1A). The content of total AMPK in all experimental groups did not differ from the values obtained in the control group (Fig. 1A).

Control animals pretreated with AICAR did not show any changes in phosphorylated acetyl-CoA carboxylase (ACC) content (Fig. 1B). In the HS group we detected a significant 34% ( $P < 0.05$ ) decrease in the content of phosphorylated ACC vs. the C group (Fig. 1B). In the HSA group the level of ACC phosphorylation did not differ from the values obtained in the C group (Fig. 1B). The content of phosphorylated ACC was higher in the HSA group as compared to the HS group. The content of total ACC did not differ between all studied groups of animals (Fig. 1B).

In the intact animals pretreated with AICAR (CA group) the content of HDAC4 in the nuclear fraction did not differ from the C group (Fig. 2A). In the HS group we observed a significant 243% increase ( $P < 0.05$ ) in the content of HDAC4 in the nuclei compared to the C group. In the HSA group the content of HDAC4 in the nuclear fraction did not differ from the C group. The nuclear HDAC4 content in the HS group was significantly higher than that in the HSA group (Fig. 2A). In the CA group we found a significant 38% decrease ( $P < 0.05$ ) in the nuclear HDAC5 content relative to the C group (Fig. 2B). In the HS group

there was a significant 41% decline ( $P < 0.05$ ) in the content of nuclear HDAC5 as compared to the C group (Fig. 2B). In the HSA group we also observed a decrease in the content of nuclear HDAC5 by 26% ( $P < 0.05$ ) relative to the C group (Fig. 2B).

AICAR pretreatment of both CA and HSA groups did not induce any changes in the content of phospho-AMPK (Ser485/491) as compared to the C group (Fig. 3A). However, when compared to the C group, in the HS group a significant 88% increase ( $P < 0.05$ ) in

phospho-AMPK (Ser485/491) was found (Fig. 3A). In line with the AMPK Ser485/491 phosphorylation, a significant 136% increase ( $P < 0.05$ ) in the content of phosphorylated protein kinase D (PKD) (Ser916) was observed only in the HS group compared to the C group (Fig. 3B).

WB and RT-PCR analyses did not reveal any significant changes in the expression of peroxisome proliferator-activated receptor  $\gamma$  coactivator 1 $\alpha$  (PGC-1 $\alpha$ ) at both protein (Fig. 4A) and mRNA levels (Fig. 4B).

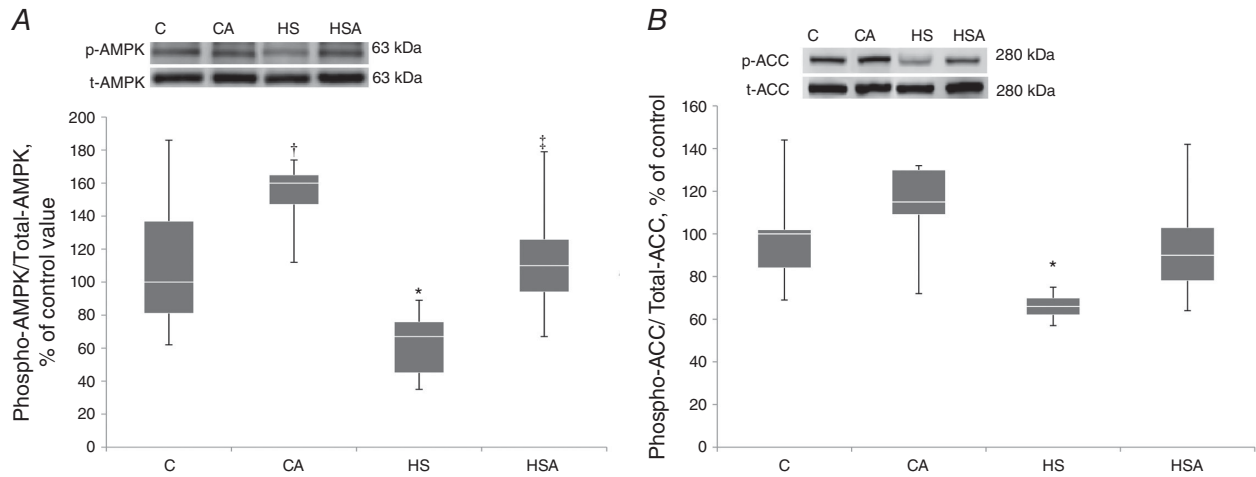


**Figure 1. Quantification of p-AMPK/t-AMPK (A) and p-ACC/t-ACC (B) ratios expressed relative (%) to control; representative immunoblots are shown above the graphs**

C, control group; CA, control with AICAR pretreatment; HS, hindlimb suspension for 24 h; HSA, hindlimb suspension for 24 h with AICAR pretreatment. \*Significant difference from control ( $P < 0.05$ ); †trend towards a significant difference from control ( $P = 0.09$ ); ‡significant difference from HS ( $P < 0.05$ ). Box plots show 25–75 percentiles and median values and the whiskers represent the minimum and the maximum;  $n = 8$ /group.

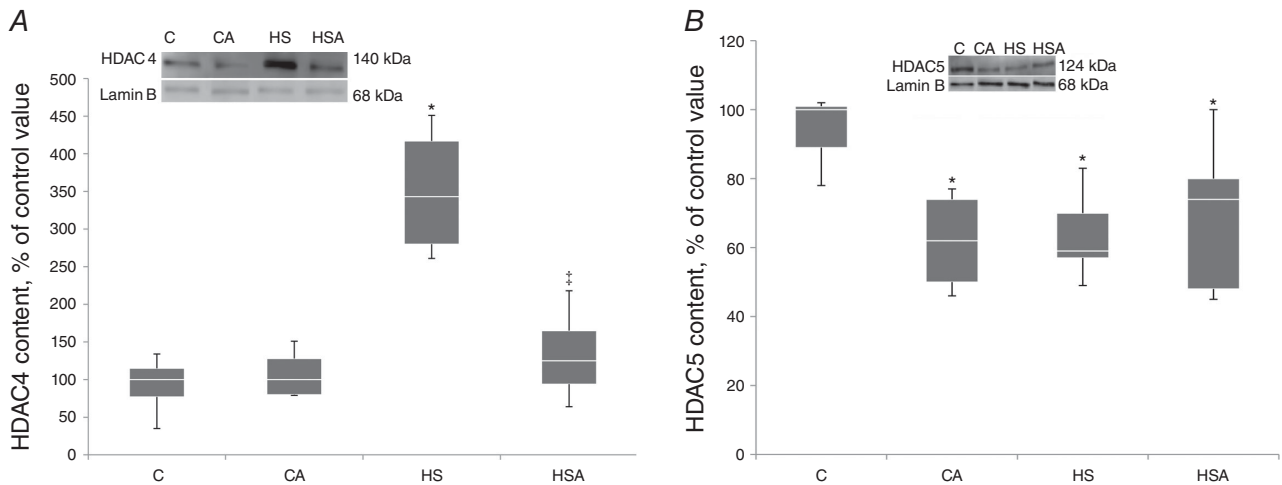


**Figure 2. Quantification of HDAC4 (A) and HDAC5 (B) in the nuclear fraction of the rat soleus expressed relative (%) to control and representative immunoblots for HDAC4 and lamin B (used for normalization)**

C, control group; CA, control with AICAR pretreatment; HS, hindlimb suspension for 24 h; HSA, hindlimb suspension for 24 h with AICAR pretreatment. \*Significant difference from control ( $P < 0.05$ ); ‡significant difference from HS ( $P < 0.05$ ). Box plots show 25–75 percentiles and median values and the whiskers represent the minimum and the maximum;  $n = 8$ /group.

The level of MyHC I( $\beta$ ) pre-mRNA expression in the CA group did not differ from the C group (Fig. 5A). In the HS group there was found a significant 0.3-fold decrease in MyHC I( $\beta$ ) pre-mRNA as compared to the C group (Fig. 5A). There was a trend ( $P = 0.09$ ) towards an increase in MyHC I( $\beta$ ) pre-mRNA in the HSA group as compared to the HS group (Fig. 5A).

In the intact animals AICAR pretreatment resulted in a significant 1.4-fold increase in the expression level of MyHC I( $\beta$ ) mRNA (Fig. 5B). In the HS group

there was a trend to a 0.2-fold decrease ( $P = 0.08$ ) in MyHC I( $\beta$ ) mRNA expression compared to the control level (Fig. 5B). In the HSA group we observed a significant 1.2-fold increase in MyHC I( $\beta$ ) mRNA as compared to the C group (Fig. 5B). There was a significant rise ( $P < 0.05$ ) in MyHC I( $\beta$ ) mRNA expression in the HSA rats relative to the HS animals (Fig. 5B).

Pretreatment of the intact animals with AICAR did not reveal any changes in MyHC IIa mRNA expression in the

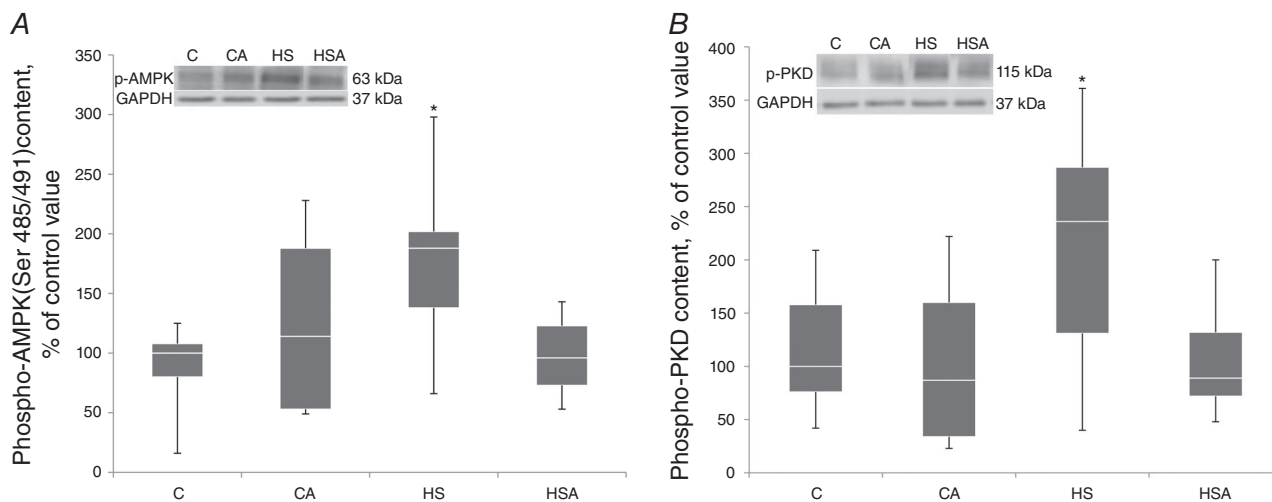


**Figure 3. Quantification of p-AMPK (Ser 485/491) (A) and p-PKD (B) in the rat soleus expressed relative (%) to control and representative immunoblots for p-AMPK (Ser 485/491) (A) and p-PKD (B) and GAPDH (used for normalization)**

C, control group; CA, control with AICAR pretreatment; HS, hindlimb suspension for 24 h; HSA, hindlimb suspension for 24 h with AICAR pretreatment. \*Significant difference from HS ( $P < 0.05$ ). Box plots show 25–75 percentiles and median values and the whiskers represent the minimum and the maximum;  $n = 8$ /group.

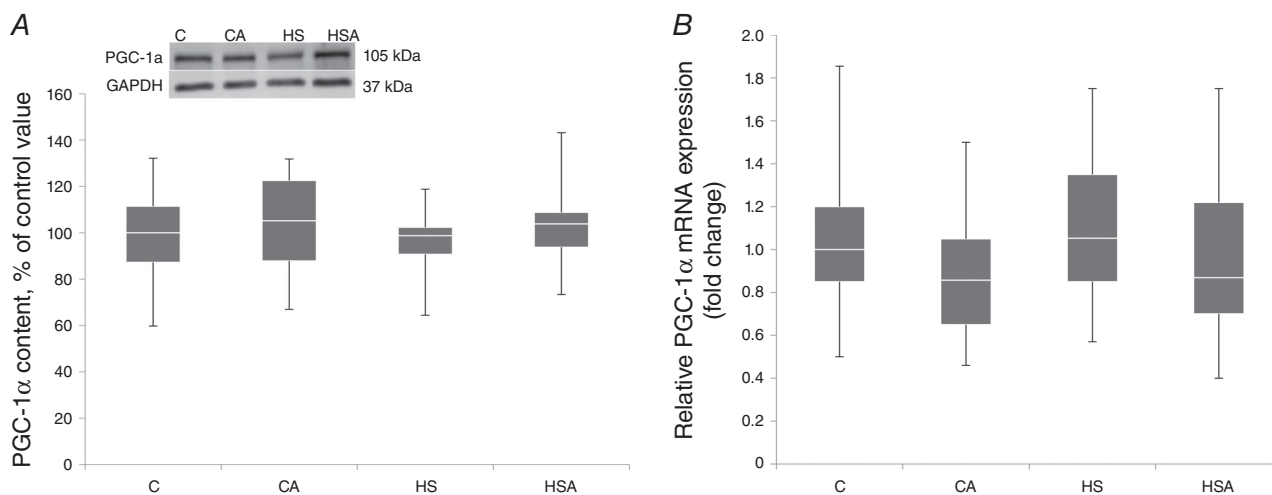


**Figure 4. PGC-1 $\alpha$  protein expression (A) and PGC-1 $\alpha$  mRNA expression (B) in the rat soleus muscle expressed relative to control**

C, control group; CA, control with AICAR pretreatment; HS, hindlimb suspension for 24 h; HSA, hindlimb suspension for 24 h with AICAR pretreatment. Box plots show 25–75 percentiles and median values and the whiskers represent the minimum and the maximum;  $n = 8$ /group.

rat soleus muscle (Fig. 6A). In the HS group there was a significant 0.4-fold decrease ( $P < 0.05$ ) in MyHC I $\alpha$  mRNA expression compared with the C group (Fig. 6A). In the HSA group the expression level of MyHC I $\alpha$  mRNA did not differ from the C group (Fig. 6A).

The AICAR-pretreated intact animals showed a significant 1.9-fold increment ( $P < 0.05$ ) in the level of MyHC I $\beta$  mRNA expression (Fig. 6B). In the HS group relative MyHC I $\beta$  mRNA expression did not differ from the C group (Fig. 6B). We also found that the level of MyHC I $\beta$  mRNA expression in the soleus of HSA rats significantly increased by 2.3-fold ( $P < 0.05$ ) in comparison with the C group (Fig. 6B). There was a significant increase ( $P < 0.05$ ) in MyHC I $\beta$  mRNA expression in HSA rats as compared to HS animals (Fig. 6B).

Hindlimb unloading for 24 h resulted in a significant 2.4-fold increase ( $P < 0.05$ ) in MyHC I $\delta/\alpha$  mRNA expression compared to the C group (Fig. 6C). In the HSA group the level of MyHC I $\delta/\alpha$  mRNA expression was significantly higher vs. both the C and HS groups (Fig. 6C).

## Discussion

The present study was aimed at identifying the role of AMPK in reducing MyHC I( $\beta$ ) mRNA expression under HU conditions. After 24-h HU we observed a significant reduction in AMPK phosphorylation in the rat soleus as

compared to control. However, HU did not induce any significant changes in total AMPK content in the soleus muscle. One day of HU also resulted in a significant decrease in phosphorylation of ACC, a specific AMPK substrate, indicating suppressed protein kinase activity of AMPK (Winder *et al.* 1997). A significant decrease in the AMPK phosphorylation level was previously reported by Han *et al.* (2007) in rat soleus after 14 days of hindlimb unloading. However, in contrast, Hilder *et al.* (2005) found an increase in AMPK phosphorylation after 14 days of unloading in rat soleus. We also observed a sufficient increase of this parameter after the same duration of unloading (unpublished observation). Egawa *et al.* (2015) reported the absence of any changes in AMPK phosphorylation and ACC phosphorylation in murine soleus after 14 days of unloading. Thus, a lot of contradictory reports were published on the AMPK phosphorylation during unloading. However all these observations were made after longer periods of unloading. No one analysed the 1-day exposure effects. As for the findings of Egawa *et al.* (2015), they were done on murine soleus muscle, which is quite different from the rat one (40–50% of slow-twitch fibres vs. 85% in rat and humans). Recently, we reported on the significant decrease in AMPK phosphorylation in rat soleus muscle after 1 and 3 days of hindlimb unloading (Mirzoev *et al.* 2016). The reduced level of AMPK phosphorylation was also found in human soleus biopsy samples after 3 days of exposure to dry immersion (Vilchinskaya *et al.* 2015).

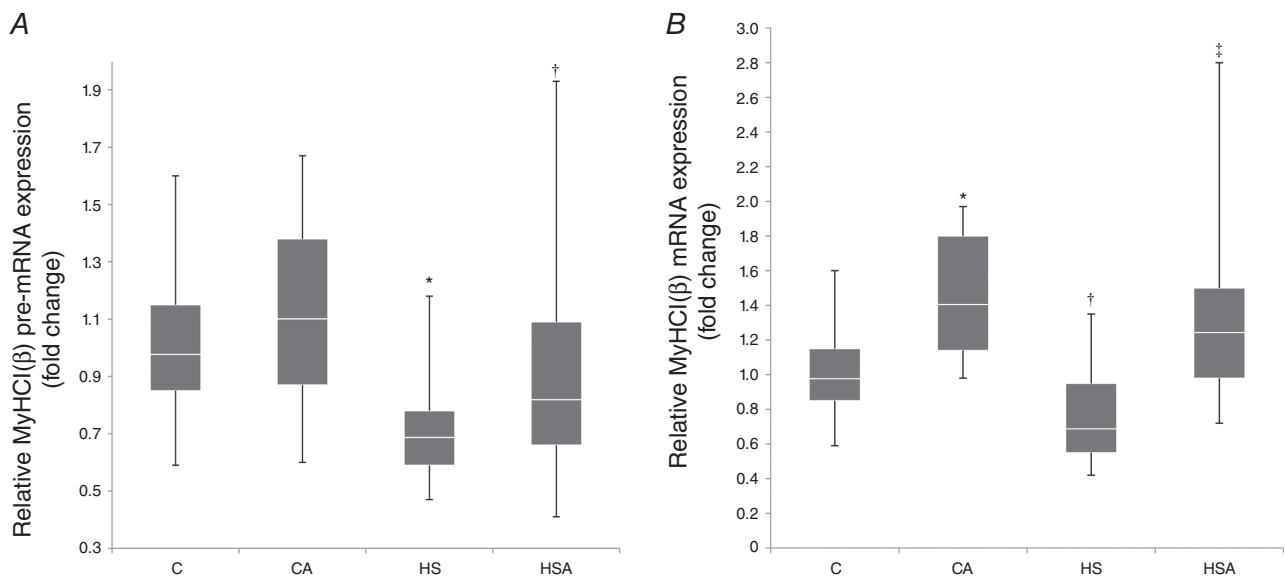


**Figure 5. Relative MyHC I( $\beta$ ) pre-mRNA (A) and mRNA (B) expression in the rat soleus muscle**  
C, control group; CA, control with AICAR pretreatment; HS, hindlimb suspension for 24 h; HSA, hindlimb suspension for 24 h with AICAR pretreatment. \*Significant difference from control ( $P < 0.05$ ); †a trend towards a significant difference from HS ( $P = 0.09$ ); ‡significant difference from HS ( $P < 0.05$ ). Box plots show 25–75 percentiles and median values and the whiskers represent the minimum and the maximum;  $n = 8$ /group.

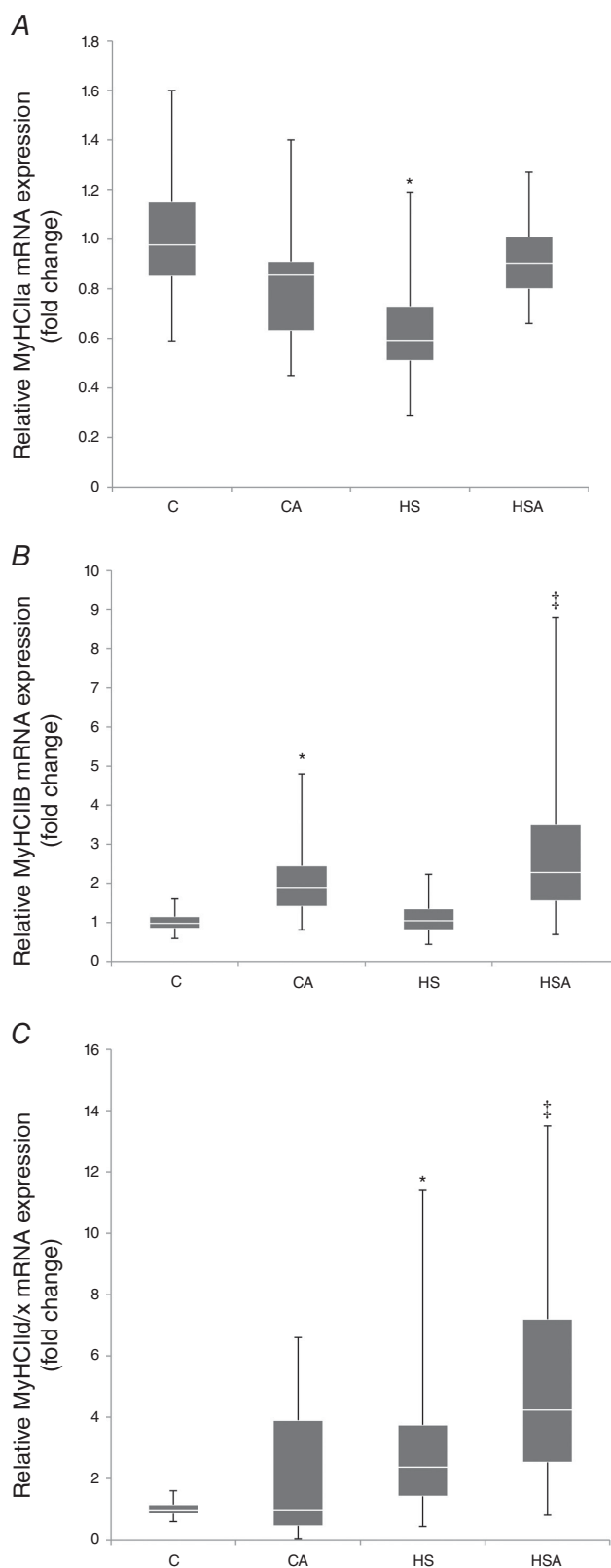


**Figure 6. Relative mRNA expression of MyHC Ila (A), MyHC IIB (B) and MyHC IId/x (C) in the rat soleus muscle**

C, control group; CA, control with AICAR pretreatment; HS, hindlimb suspension for 24 h; HSA, hindlimb suspension for 24 h

In order to study the role of AMPK in the regulation of the myosin phenotype in the soleus muscle fibres at the early stage of mechanical unloading as well as to analyse the signalling consequences of AMPK dephosphorylation, a well-known AMPK activator, AICAR, has been used. Pretreatment of the intact animals with AICAR resulted in a non-significant increase in AMPK and ACC phosphorylation in the rat soleus muscle compared to the untreated control. Previously it was shown that AICAR administration does not lead to a significant increase in AMPK activity in rat soleus muscle (Zheng *et al.* 2001). Our data are in agreement with this report. At the same time, the results of our study show that pretreatment with AICAR for 6 days before HU and during 24-h HU did prevent AMPK dephosphorylation in the rat soleus muscle following a period of 24-h HU. AICAR pretreatment also rescued ACC dephosphorylation after 1-day HU. Thus, we, for the first time, were able to prevent a decrease in AMPK activity during the first day of unloading. If our hypothesis about the role of AMPK in the regulation of MyHC I (*myh7*) expression is true, then we could expect that AICAR-induced AMPK activity would prevent a decrease in MyHC I mRNA following 24-h HU. We found a significant decrease in MyHC I( $\beta$ ) pre-mRNA and a pronounced trend towards a decrease in MyHC I( $\beta$ ) mature mRNA I( $\beta$ ) following an exposure to 24-h HU (Fig. 5). These data are in a good agreement with the report by Giger *et al.* (2009) about a significant reduction in both pre-mRNA and mature mRNA of slow-type MyHC in the soleus muscle of female Sprague–Dawley rats following 1-day HU. However, AICAR pretreatment rescued a decrease in MyHC I( $\beta$ ) pre-mRNA in the soleus muscle of the unloaded rats. Anyway, various authors reported a decrease in MyHC I( $\beta$ ) mRNA content from the first to the 14th day of HU (Stevens *et al.* 1999; Giger *et al.* 2009; Lomonosova *et al.* 2016). We recently demonstrated that p-AMPK and p-ACC gradually increased in the course of HU exposure, and therefore after the first 1–3 days of HU one could not expect further dependence of MyHC I( $\beta$ ) mRNA decline on AMPK dephosphorylation. Indeed, we observed some signs of the fact that after the third day, the calcineurin inhibitor (calsarcin-2) expression and NFATc1 kinase GSK3 $\beta$  dephosphorylation/activation were intensified (Lomonosova *et al.* 2016). It seems quite reasonable to suppose that at the later stage of the exposure to HU, mechanisms other than AMPK signalling are responsible for MyHC I( $\beta$ ) mRNA decline.

with AICAR pretreatment. \*Significant difference from control ( $P < 0.05$ ); †significant difference from HS ( $P < 0.05$ ). Box plots show 25–75 percentiles and median values and the whiskers represent the minimum and the maximum;  $n = 8/\text{group}$ .



One possible effect of AMPK on gene expression of slow myosin and enzymes of oxidative metabolism is associated with the phosphorylation/dephosphorylation of histone deacetylase 4 and 5 (HDAC4 and HDAC5) (Röckl *et al.* 2007; McGee & Hargreaves, 2010). We hypothesized that AMPK dephosphorylation at the first day of HU would lead to an accumulation of HDAC4 and 5 in the nuclear fraction of the rat soleus muscle. This hypothesis is supported by the previous studies on histone H3 acetylation. Pandorf *et al.* (2009) found a profound decrease in acetylated histone linked with the *myh7* gene promoter after 7 days of HU. In addition, it has been previously shown that in slow-type muscle fibres, HDAC4 is localized predominantly in the cytoplasm, and in fast-type fibres, in the nuclei (Cohen *et al.* 2015). Indeed, we detected a significant accumulation of HDAC4 in the nuclear fraction of the soleus muscle after 24-h unloading while AMPK activation with AICAR prevented such accumulation. This is consistent with the data on AMPK phosphorylation and confirms our hypothesis. Recently, Yoshihara *et al.* (2016) have found that 10 days of immobilization induces a significant nuclear HDAC4 accumulation in rat gastrocnemius muscle. This HDAC4 accumulation was accompanied by a decrease in the level of AMPK phosphorylation (Yoshihara *et al.* 2016). These data are in accord with the results of our experiment.

As for HDAC5, we observed that even a slight increase in the activity of AMPK in the CA group was accompanied by a decrease in HDAC5 content in the nuclear fraction. This phenomenon could be linked to the phosphorylation of HDAC5 under the action of AMPK. However, surprisingly, we found a decrease in the content of HDAC5 in the nuclear fraction after 24 h of unloading. Such a decrease could be caused either by HDAC5 phosphorylation and export from the nuclei or by HDAC5 degradation. HDAC5 is not only an AMPK target, but also a target for PKD (Ya & Rubin, 2011; McGee *et al.* 2014). Because 24-h HS resulted in a decrease in the AMPK activity, it is unlikely that the export of HDAC5 from the nucleus during unloading could be linked to AMPK. It is known that a decrease in the AMPK activity can lead to a significant increase in the PKD phosphorylation level (McGee *et al.* 2014). Indeed, we observed a significant increase in the phosphorylation level of PKD in the HS group, but not in the HSA group. Interestingly, this decrease in PKD phosphorylation in the HSA group attenuated a reduction in HDAC5 in the nuclear fraction by almost 2-fold. It is important to note that an increase in PKD phosphorylation in the HS group had no impact on nuclear HDAC4, the content of which was significantly higher than that in the C group. It appears that HDAC4 is not a target for PKD during mechanical unloading. In the present study, we for the first time observed a reciprocal relationship between AMPK and PKD in the inactivated rat soleus muscle. In addition, hindlimb unloading resulted in a significant increase in AMPK Ser485/491 phosphorylation, which is under control of PKD (Coughlan *et al.* 2016). However, an allosteric activation of AMPK with AICAR in the HSA group reduced the level of AMPK Ser485/491 phosphorylation, possibly, through decreased PKD phosphorylation. Because HDAC5 and HDAC4 are associated with deacetylation of both histone H3 and transcription factor MEF2D (a promoter of activity of several genes, including *myh7*) (Shen *et al.* 2006), we speculate that the increased activity of PKD as well as HDAC5 nuclear export during unloading would attenuate a decrease in MyHC I( $\beta$ ) expression.

Interestingly, 24-h HU also induced a reduction in MyHC IIa mRNA expression. This result conforms to a report by Stevens *et al.* (1999) as well as our recent study (Lomonosova *et al.* 2016) that showed a significant decline in MyHC IIa mRNA expression in rat soleus at the early stages of HU. In the present study we observed a similar expression pattern for MyHC I and MyHC IIa mRNAs during an acute unloading. Therefore, we can suggest that MyHC IIA mRNA expression might be regulated via the same mechanisms as that for MyHC I, i.e. calcineurin/NFAT-dependent and AMPK-dependent signalling cascades. Indeed, in the AICAR-pretreated rats we did not observe a decrease in MyHC IIA mRNA following HU. It is possible that nuclear HDAC4 accumulation after

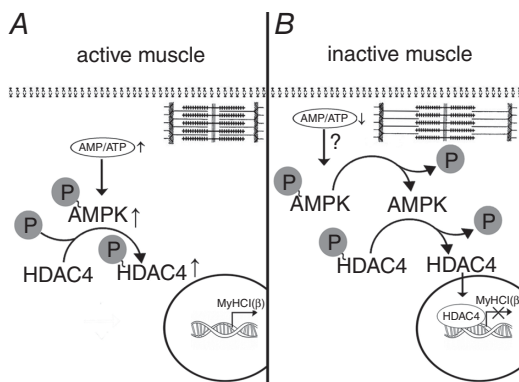


**Figure 7. A schematic representation depicting a hypothetical mechanism of the AMPK influence on MyHC I( $\beta$ ) mRNA expression via HDAC4 in an active and unloaded rat soleus muscle**

*A*, rat soleus muscle under the conditions of normal activity. Normal contractile activity determines an equilibrium in the AMP:ATP ratio when the level of AMPK phosphorylation maintains an equilibrium in the level of HDAC4 phosphorylation, the main pool of which is localized in the cytoplasm (Cohen *et al.* 2015). No blocking of the promoter of the *myh7* gene occurs and MyHC I( $\beta$ ) mRNA is expressed normally. *B*, rat soleus muscle under the unloading conditions. Sharply reduced contractile activity may lead to an accumulation of ATP and reduction in AMP. As a result, the level of AMPK phosphorylation decreases and induces partial HDAC4 dephosphorylation and its nuclear translocation. The *myh7* gene promoter gets blocked and MyHC I( $\beta$ ) mRNA expression decreases.

1 day of unloading could be the cause of the decline in MyHC IIA mRNA expression. Earlier it had been shown that during the first days of HU a significant increase in MyHC IId/x mRNA expression occurs (Stevens *et al.* 1999; Lomonosova *et al.* 2016). In the present study we also observed a significant rise in MyHC IId/x mRNA after 24-h HU while AICAR pretreatment enhanced MyHC IId/x mRNA expression in the HSA group compared to the HS group. It is worth noting that an increase in MyHC IId/x mRNA expression after 24-h unloading occurred against the background of AMPK dephosphorylation and nuclear HDAC4 accumulation, which could non-specifically prevent transcriptional activity. Presumably, the increased MyHC IId/x mRNA expression is a consequence of other mechanisms which are not associated with the changes in AMPK kinase activity. However, it is possible that an overall activation of transcriptional activity in the AICAR-pretreated unloaded animals could enhance MyHC IId/x mRNA expression.

Stevens *et al.* (1999) and Lomonosova *et al.* (2016) have previously shown that 3–4 days of unloading can lead to an increase in MyHC IIB mRNA expression. However, in the present study, 24-h HU was not sufficient to induce any significant changes in MyHC IIB mRNA expression. At the same time, an export of HDAC4 from the nuclei in the AICAR-pretreated unloaded rats could create some conditions for enhanced MyHC IIB mRNA expression.

There is evidence indicating that PGC-1 $\alpha$  may play a key role in mitochondrial biogenesis, fatty acid oxidation as well as muscle fibre type determination (Lin *et al.* 2002; Miura *et al.* 2003). This allowed us to assume that PGC-1 $\alpha$  could lie downstream of AMPK and influence skeletal muscle phenotype. In addition, Cannavino *et al.* (2014) have shown that 3 days of HU results in a significant reduction in PGC-1 $\alpha$  mRNA expression in mouse soleus muscle. In this regard, one of the aims of the present study was to examine whether AMPK activity could exert an impact on PGC-1 $\alpha$  mRNA and protein expression following 24-h unloading. We found that 24-h HU did not induce any significant changes in PGC-1 $\alpha$  expression (both mRNA and protein) in rat soleus muscle. Activation of AMPK with AICAR also did not alter PGC-1 $\alpha$  expression in both intact and unloaded rats. These data suggest that PGC-1 $\alpha$  expression in rat soleus muscle during the initial stage of unloading (24 h) is not regulated by AMPK activity and therefore cannot influence an expression pattern of MyHC isoforms. It is also possible that AMPK dephosphorylation may participate in other events during the early period of mechanical unloading: paradoxical increase in ribosomal protein S6 kinase (p70S6K) phosphorylation (Mirzoev *et al.* 2016) or inactivation of the  $\alpha 2$  subunit of Na<sup>+</sup>,K<sup>+</sup>-ATPase (Kravtsova *et al.* 2016).

## Conclusion

The results of the present study clearly indicate that AMPK dephosphorylation during the first 24 h of mechanical unloading has a significant impact on the expression of MyHC isoforms in rat soleus causing a decrease in MyHC I( $\beta$ ) pre-mRNA and mRNA expression as well as MyHC IIA mRNA expression. Dephosphorylation of AMPK also contributes to HDAC4 nuclear translocation suggesting an important role of this epigenetic regulator in the process of myosin phenotype transformation (Fig. 7).

## References

- Cannavino J, Brocca L, Sandri M, Bottinelli R & Pellegrino MA (2014). PGC1- $\alpha$  over-expression prevents metabolic alterations and soleus muscle atrophy in hindlimb unloaded mice. *J Physiol* **592**, 4575–4589.
- Cohen TJ, Choi MC, Kapur M, Lira VA, Yan Z & Yao TP (2015). HDAC4 regulates muscle fibre type-specific gene expression programs. *Mol Cells* **38**, 343–348.
- Coughlan KA, Valentine RJ, Sudit BS, Allen K, Dagon Y, Kahn BB, Ruderman NB & Saha AK (2016). PKD1 inhibits AMPK $\alpha 2$  through phosphorylation of serine 491 and impairs insulin signalling in skeletal muscle cells. *J Biol Chem* **291**, 5664–5675.
- De-Doncker L, Kasri M, Picquet F & Falempin M (2005). Physiologically adaptive changes of the L5 afferent neurogram and of the rat soleus EMG activity during 14 days of hindlimb unloading and recovery. *J Exp Biol* **208**, 4585–4592.
- Dupré-Aucouturier S, Castells J, Freyssenet D & Desplanches D (2015). Trichostatin A, a histone deacetylase inhibitor, modulates unloaded induced skeletal muscle atrophy. *J Appl Physiol* **119**, 342–351.
- Egawa T, Goto A, Ohno Y, Yokoyama S, Ikuta A, Suzuki M, Sugiura T, Ohira Y, Yoshioka T, Hayashi T & Goto K (2015). Involvement of AMPK in regulating slow-twitch muscle atrophy during hindlimb unloading in mice. *Am J Physiol Endocrinol Metab* **309**, E651–E662.
- Giger JM, Bodell PW, Zeng M, Baldwin KM & Haddad F (2009). Rapid muscle atrophy response to unloading: pretranslational processes involving MHC and actin. *J Appl Physiol* (1985) **107**, 1204–1212.
- Grundy D (2015). Principles and standards for reporting animal experiments in *The Journal of Physiology* and *Experimental Physiology*. *J Physiol* **593**, 2547–2549.
- Han B, Zhu MJ, Ma C & Du M (2007). Rat hindlimb unloading down-regulates insulin like growth factor-1 signalling and AMP-activated protein kinase, and leads to severe atrophy of the soleus muscle. *Appl Physiol Nutr Metab* **32**, 1115–1123.
- Hilder TL, Baer LA, Fuller PM, Fuller CA, Grindeland RE, Wade CE & Graves LM (2005). Insulin-independent pathways mediating glucose uptake in hindlimb-suspended skeletal muscle. *J Appl Physiol* (1985) **99**, 2181–2188.

- Kravtsova VV, Petrov AM, Matchkov VV, Bouzinova EV, Vasiliev AN, Benziane B, Zefirov AL, Chibalin AV, Heiny JA & Krivoi II (2016). Distinct  $\alpha 2$  Na,K-ATPase membrane pools are differently involved in early skeletal muscle remodeling during disuse. *J Gen Physiol* **147**, 175–188.
- Lin J, Wu H, Tarr PT, Zhang CY, Wu Z, Boss O, Michael LF, Puigserver P, Isotani E, Olson EN, Lowell BB, Bassel-Duby R & Spiegelman BM (2002). Transcriptional co-activator PGC-1 $\alpha$  drives the formation of slow twitch muscle fibres. *Nature* **418**, 797–801.
- Liu W, Chen G, Li F, Tang C & Yin D (2014). Calcineurin-NFAT signalling and neurotrophins control transformation of myosin heavy chain isoforms in rat soleus muscle in response to aerobic treadmill training. *J Sports Sci Med* **13**, 934–944.
- Liu Y, Randall WR & Schneider MF (2005). Activity-dependent and -independent nuclear fluxes of HDAC4 mediated by different kinases in adult skeletal muscle. *J Cell Biol* **168**, 887–897.
- Livak KJ & Schmittgen TD (2001). Analysis of relative gene expression data using real-time quantitative PCR and the  $2^{(-\Delta\Delta C(T))}$  method. *Methods* **25**, 402–408.
- Lomonosova YN, Turtikova OV & Shenkman BS (2016). Reduced expression of MyHC slow isoform in rat soleus during unloading is accompanied by alterations of endogenous inhibitors of calcineurin/NFAT signalling pathway. *J Muscle Res Cell Motil* **37**, 7–16.
- Matoba T, Wakatsuki Y & Ohira Y (1993).  $\beta$ -Guanidinopropionic acid suppresses suspension-induced changes in myosin expression in rat skeletal muscle. *Med Sci Sports Exerc* **25**, 157.
- McGee SL & Hargreaves M (2010). AMPK-mediated regulation of transcription in skeletal muscle. *Clin Sci (Lond)* **118**, 507–518.
- McGee SL, Swinton C, Morrison S, Gaur V, Campbell DE, Jorgensen SB, Kemp BE, Gregory KB, Steinberg R & Hargreaves M (2014). Compensatory regulation of HDAC5 in muscle maintains metabolic adaptive responses and metabolism in response to energetic stress. *FASEB J* **28**, 3384–3395.
- Mirzoev T, Tyganov S, Vilchinskaya N, Lomonosova Y & Shenkman B (2016). Key markers of mTORC1-dependent and mTORC1-independent signalling pathways regulating protein synthesis in rat soleus muscle during early stages of hindlimb unloading. *Cell Physiol Biochem* **39**, 1011–1020.
- Miura S, Kai Y, Ono M & Ezaki O (2003). Overexpression of peroxisome proliferator-activated receptor gamma coactivator-1 $\alpha$  down-regulates GLUT4 mRNA in skeletal muscles. *J Biol Chem* **278**, 31385–31390.
- Morey-Holton E & Globus R (2002). Hindlimb unloading rodent model: technical aspects. *J Appl Physiol* **92**, 1367–1377.
- Mounier R, Th  ret M, Lantier L, Foretz M & Viollet B (2015). Expanding roles for AMPK in skeletal muscle plasticity. *Trends Endocrinol Metab* **26**, 275–286.
- Pandorf CE, Haddad F, Wright C, Bodell PW & Baldwin KM (2009). Differential epigenetic modifications of histones at the myosin heavy chain genes in fast and slow skeletal muscle fibres and in response to muscle unloading. *Am J Physiol Cell Physiol* **297**, C6–C16.
- Pette D & Staron RS (2001). Transitions of muscle fibre phenotypic profiles. *Histochem Cell Biol* **115**, 359–372.
- Putman CT, Gallo M, Martins KJ, MacLean IM, Jendral MJ, Gordon T, Syrotuik DG & Dixon WT (2015). Creatine loading elevates the intracellular phosphorylation potential and alters adaptive responses of rat fast-twitch muscle to chronic low-frequency stimulation. *Appl Physiol Nutr Metab* **40**, 671–682.
- R  ckl KS, Hirshman MF, Brandauer J, Fujii N, Witters LA & Goodyear LJ (2007). Skeletal muscle adaptation to exercise training: AMP-activated protein kinase mediates muscle fibre type shift. *Diabetes* **56**, 2062–2069.
- Shen T, Cseresny  s Z, Liu Y, Randall WR & Schneider MF (2007). Regulation of the nuclear export of the transcription factor NFATc1 by protein kinases after slow fibre type electrical stimulation of adult mouse skeletal muscle fibres. *J Physiol* **579**, 535–551.
- Shen T, Liu Y, Randall WR & Schneider MF (2006). Parallel mechanisms for resting nucleocytoplasmic shuttling and activity dependent translocation provide dual control of transcriptional regulators HDAC and NFAT in skeletal muscle fibre type plasticity. *J Muscle Res Cell Motil* **27**, 405–411.
- Stevens L, Sultan KR, Peuker H, Gohlsch B, Mounier Y & Pette D (1999). Time-dependent changes in myosin heavy chain mRNA and protein isoforms in unloaded soleus muscle of rat. *Am J Physiol Cell Physiol* **277**, C1044–C1049.
- Vilchinskaya NA, Mirzoev TM, Lomonosova YN, Kozlovskaya IB & Shenkman BS (2015). Human muscle signalling responses to 3-day head-out dry immersion. *J Musculoskelet Neuronal Interact* **15**, 286–293.
- Winder WW, Wilson HA, Hardie DG, Rasmussen BB, Hutber CA, Call GB, Clayton RD, Conley LM, Yoon S & Zhou B (1997). Phosphorylation of rat muscle acetyl-CoA carboxylase by AMP-activated protein kinase and protein kinase A. *J Appl Physiol* **82**, 219–225.
- Ya F & Rubin CS (2011). Protein kinase D: coupling extracellular stimuli to the regulation of cell physiology. *EMBO Rep* **12**, 785–796.
- Yoshihara T, Machida S, Kurosaka Y, Kakigi R, Sugiura T & Naito H (2016). Immobilisation induces nuclear accumulation of HDAC4 in rat skeletal muscle. *J Physiol Sci* **66**, 337–343.
- Zheng D, Maclean P, Pohnert SC, Knight JB, Olson AL, Winder WW & Dohm GL (2001). Regulation of muscle GLUT-4 transcription by AMP-activated protein kinase. *J Appl Physiol (1985)* **91**, 1073–1083.
- Zong H, Ren JM, Young LH, Pypaert M, Mu J, Birnbaum MJ & Shulman GI (2002). AMP kinase is required for mitochondrial biogenesis in skeletal muscle in response to chronic energy deprivation. *Proc Natl Acad Sci USA* **99**, 15983–15987.

## Additional information

### Competing interests

The authors declare no competing interests.

### Author contributions

Experiments were carried out at the Myology Laboratory, Institute of Biomedical problems of the Russian Academy of Sciences. The authors contributed to the paper as follows: N.A.V. and B.S.S. designed the study; N.A.V., E.P.M. and O.V.T. performed the experiments; N.A.V., T.M.M., T.L.N. and B.S.S. analysed and interpreted the data, and wrote the manuscript. All authors have approved the final version of the manuscript and agree to be accountable for all aspects of the work. All persons designated as authors qualify for authorship, and all those who qualify for authorship are listed.

### Funding

The study was supported by the Russian Science Foundation grant no. 14-15-00358.

### Acknowledgements

The authors thank Dr Yulia Lomonosova and Dr Svetlana Belova for excellent methodological assistance.